From APS to HVOF spraying of conventional and nanostructured titania feedstock powders : A study on the enhancement of the mechanical properties

Lima, R. S.; Marple, B. R.

Publisher's version / Version de l'éditeur:
https://doi.org/10.1016/j.surfcoat.2004.10.137
Surface & Coatings Technology, 200, 11, pp. 3428-3437, 2006-03-15

Available online at www.sciencedirect.com

SCIENCE DIRECT

Surface & Coatings Technology 200 (2006) 3428–3437

SURFACE & COATINGS TECHNOLOGY

www.elsevier.com/locate/surfcoat

From APS to HVOF spraying of conventional and nanostructured titania feedstock powders: a study on the enhancement of the mechanical properties

R.S. Lima*, B.R. Marple

National Research Council of Canada, Boucherville, QC J4B 6Y4, Canada

Received 3 August 2004; accepted in revised form 28 October 2004
Available online 20 December 2004

Abstract

Nanostructured and conventional titania (TiO_2) feedstocks were thermal sprayed using air plasma spray (APS) and high-velocity oxy-fuel (HVOF). The HVOF-sprayed coatings made from the nanostructured feedstock exhibited superior abrasion resistance, bond strength and crack propagation resistance when compared to the coatings made from the conventional feedstocks sprayed using HVOF and APS. The enhancement of the mechanical properties was due to (i) the processing (HVOF) and (ii) the nanocharacter of the feedstock. It was found that the HVOF-sprayed coating made from the nanostructured feedstock exhibited isotropic characteristics and microstructure with tiny zones of agglomerated nanostructured particles randomly spread throughout the coating structure. It was observed that these nanostructured zones acted as crack arresters by blunting and branching crack tips, enhancing the crack propagation resistance of the coating. Due to the isotropic characteristics of mechanical properties, the HVOF-sprayed coating made from the nanostructured feedstock exhibited uniform crack propagation under Vickers indentation, i.e., four cracks emanating from the corners of the Vickers indentation impression.

Keywords: Abrasive wheel test; Bond strength test (ASTM C633); Scanning electron microscopy (SEM); Thermal spraying; Titanium oxide; Nanostructured coating

1. Introduction

Titania or titanium dioxide (TiO_2) thermal spray coatings have been employed for many years in antiwear applications, e.g., in the propeller shaft-bearing sleeve of boats and pump seals where they must resist contact with abrasive grains and hard surfaces [1]. These titania coatings have been extensively applied via air plasma spray (APS), the traditional method of depositing ceramic thermal spray coatings. To produce these titania coatings, conventional titania feedstock powders, generally fused and crushed, have been traditionally employed.

The APS approach has normally been used to deposit TiO_2 because of the high plasma temperatures (up to ~14,000 °C) of the plasma spray torches [2], which are high enough to melt ceramic materials. However, because of its relatively low melting point (1855 °C) [3], titania can also be sprayed via the high-velocity oxy-fuel (HVOF) process [4,5], which normally exhibits low flame temperatures (<3000 °C) but high particle velocities [2,4,5]. It is important to point out that HVOF torches were originally engineered to spray metals and cermets, not ceramics.

Recently, the scientific community has focused considerable attention on nanostructured materials. It has been demonstrated that nanomaterials can exhibit enhanced hardness, strength, ductility and toughness when compared to their conventional counterparts [6–8]. These characteristics open interesting possibilities in thermal spray. Indeed, it has already been shown that nanostructured thermal spray ceramic oxide coatings, like Al_2O_3–TiO_2 and TiO_2, can have a superior wear performance when compared to similar coatings produced from conventional ceramic oxide pow-

* Corresponding author. Tel.: +1 450 641 5150; fax: +1 450 641 5105.
E-mail address: rogerio.lima@cnrc-nrc.gc.ca (R.S. Lima).

0257-8972/$ - see front matter © 2004 Elsevier B.V. All rights reserved.
doi:10.1016/j.surfcoat.2004.10.137

ders [9–11]. However, in other cases, authors have not observed this same improvement in the wear behavior when using nanostructured feedstocks [12].

Liu et al. [12] sprayed conventional alumina–titania feedstocks via APS and HVOF and a nanostructured alumina–titania feedstock via APS. The air plasma-sprayed coatings made from nanostructured and conventional feedstock powders exhibited the same abrasion resistance; however, the HVOF-sprayed coating made from a conventional feedstock exhibited a 100% higher abrasion resistance when compared to the air plasma-sprayed coatings. Therefore, it may be stated that the processing had a much greater influence on the abrasion behavior than the structure of the feedstock. However, no alumina–titania nanostructured feedstock powders were HVOF-sprayed for a final evaluation.

It was observed that HVOF-sprayed titania coatings made from conventional feedstock powders exhibited high hardness, low porosity (<1%), highly uniform microstructures and high Weibull modulus values [4,5]. These characteristics of the HVOF-sprayed ceramic coatings could contribute to producing an improved performance in wear resistance and may help explain why Liu et al. [12] observed a superior abrasion resistance in an HVOF-sprayed alumina–titania coating.

The objective of this study was to further investigate and compare the use of APS and HVOF for depositing ceramics by spraying conventional titania feedstock powders. The air plasma spray process represents the current and traditional method of ceramic coating application, whereas the HVOF technique represents the alternative for applying this type of material. For a final comparison and evaluation, a nanostructured titania feedstock was HVOF-sprayed, and the mechanical properties and performance of this coating were compared to those of the conventional ones. It was hoped that the HVOF character of the ceramic coating (i.e., high density and uniformity), in combination with the nanostructural character of the feedstock, would produce coatings with an optimal mechanical performance.

2. Experimental procedure

2.1. Feedstocks

One nanostructured and two conventional titania feedstocks were employed in this work. The nanostructured titania feedstock (VHP-DCS (5–20 μm), Altair Nanomaterials, Reno, NV, USA) was agglomerated and sintered and exhibited a nominal particle size range from 5 to 20 μm. The conventional titania feedstocks were fused and crushed. One (Flomaster 22.8(99)F4, F. J. Brodmann and Co., Harvey, LA, USA) had a nominal particle size range from 5 to 20 μm and the other (Metco 102, Sulzer-Metco, Westbury, NY, USA) from 7.8 to 88 μm.

2.2. Thermal spraying

The combination of torches and feedstocks employed in this work are listed in Table 1. For HVOF spraying, various O_2/propylene flow ratios were initially tested by monitoring particle temperature using a diagnostic tool (DPV 2000, Tecnar Automation, Saint Bruno, QC, Canada). The parameter set that produced the highest average particle temperature for each of the two feedstocks was selected for coating production. The air plasma-sprayed coating was produced based on the spray parameters recommended by the manufacturer of the torch and feedstock (Sulzer-Metco), and the particle temperature and velocity in the plasma jet were also monitored. For each spraying case, a total of 5000 particles were measured at the centerline of the spray jet where the particle flow density was the highest. The particle detector was placed at the same spray distance as used when depositing the coatings.

During the spraying process, a cooling system (air jets) was applied to reduce the coating temperature, which was monitored using a single color pyrometer (wave lengths, 8–12 μm; temperature range, 0–500 °C). The pyrometer was previously calibrated (emissivity) by using a reference titania coating. The maximum temperature for the air plasma-sprayed coating was approximately 150 °C, whereas, for the HVOF-sprayed coatings, it was approximately 270 °C.

2.3. Nanostructure, microstructure and porosity

The nanostructural features of the titania feedstock VHP-DCS (5–20 μm) and its HVOF-sprayed coating were analyzed via scanning electron microscopy (SEM). The overall coating microstructure and porosity of all coatings were also analyzed via SEM and image analysis. A total of five images per coating were analyzed to determine the porosity levels.

X-ray diffraction (XRD; Cu Kα radiation) was used to determine the phases present in the coatings. A 2θ diffraction angle ranging from 20–80° (using a step size of 0.05° and step time of 2.5 s) was employed.

2.4. Microhardness and crack propagation resistance

Vickers microhardness measurements were performed under a 300-g load for 15 s on the cross-section of the coatings. A total of 10 microhardness measurements were

Table 1
Processes and torches employed for spraying nanostructured and conventional feedstock powders

Titania feedstock	Process–Torch
Nanostructured VHP-DCS (5–20 μm)	HVOF–DJ2700-hybrid[a]
Conventional Flomaster 22.8(99)F4	HVOF–DJ2700-hybrid[a]
Conventional Metco 102	APS–F4-MB[a]

[a] Sulzer-Metco, Westbury, NY, USA.

carried out for each coating. The crack propagation resistance was determined by indenting the coating cross-section with a Vickers indenter at a 5-kg load for 15 s, with the indenter aligned such that one of its diagonals would be parallel to the substrate surface. The total length of the major crack ($2c$) parallel to the substrate surface that originated at or near the corners of the Vickers indentation impression was measured. Based on the indentation load (P) and $2c$, the crack propagation resistance was measured according to the relation between load and crack length $P/c^{3/2}$ [13], where P is in Newtons, and c is in meters. All indentation cracks were significantly larger than the diagonal length of the indentation impression ($2a$), i.e., $c \geq 2a$. Therefore, it is assumed that these cracks had halfpenny geometry [13]. All the indentations were performed very near the center-line of the cross-section, and the average of five indentations was taken for crack propagation resistance calculations.

2.5. Abrasion resistance and bond strength

The abrasion resistance of the coatings was tested based on the ASTM standard G65-00 (procedure D-modified) [14] also known as the dry sand/rubber wheel test. In this test, a stationary coated sample was pressed against a rotating rubber-coated wheel (228.6 mm in diameter—200 rpm) with a force of 45 N. Silica sand (212–300 μm) was fed (300–400 g/min) between the coating and rubber wheel until the wheel traveled over the equivalent linear distance of 1436 m. Prior to being submitted to this test, the surfaces of the coatings were prepared by grinding with diamond wheels to produce a surface finish R_a~0.23 μm. Two samples were tested for each of the three different coating types produced in the study. The volume of the material abraded away during the test was measured via optical profilometry.

The bond strength of the coatings was tested using the ASTM standard C 633-01 for determining the adhesion or cohesion strength of thermal spray coatings [15]. A total of five samples were tested for each of the three different coating types produced in this study.

The coatings for the abrasion test were sprayed on low carbon steel substrates (length, 76.2 mm; width, 25.4 mm; thickness, 12.7 mm) that had been grit blasted before spraying. The coating thicknesses were approximately 530–580 μm. The coatings for the bond strength test were also sprayed on low carbon steel substrates that had been grit blasted to roughen the surface before spraying. The coating thicknesses ranged from 390–450 μm.

2.6. Residual stress

To obtain some qualitative information on the residual stress condition of the coatings, an Almen strip (type N; grade I; Electronics Inc., Mishawaka, IN, USA) was mounted alongside the abrasion test substrates and coated during the spraying process. The deflection of the Almen strip was read via an Almen gage (Model TSP-3, Electronics Inc.) before and after the coating deposition. The difference between these two values indicated whether the coating was in compression (negative value) or tension (positive value). This Almen procedure was based on a technique described by Ref. [16].

3. Results and discussion

3.1. Nanostructured titania feedstock

Figs. 1 and 2 show the morphology of the nanostructured feedstock. Fig. 1 shows the SEM picture of typical particles of titania of the VHP-DCS (5–20 μm) feedstock. They are microscopic and exhibit the typical characteristics of spray-dried particles (e.g., spherical geometry and "donut shape"); however, when the cross-section of these particles is analyzed at high magnification (e.g., 60,000×), it is possible to observe the nanostructure (Fig. 2). Each particle is formed by the agglomeration of individual nanosized titania particles with diameters smaller than 100 nm.

During the spraying process, part of the nanostructured ceramic feedstock will have to be melted to assure coating integrity, i.e., adhesion and cohesion. In thermal spray coatings made from nanostructured feedstocks, the non-molten feedstock particles are surrounded by the particles that were melted during the spraying process. These previously molten particles act as a binder, maintaining coating integrity. It is important to point out that ceramic materials exhibit negligible plastic deformation; therefore, it is expected that most particles with temperatures lower than that of their melting point will bounce off the substrate surface [17].

3.2. In-flight particle characteristics

The results of particle temperature and velocity are shown in Fig. 3. It can be observed that that the HVOF-

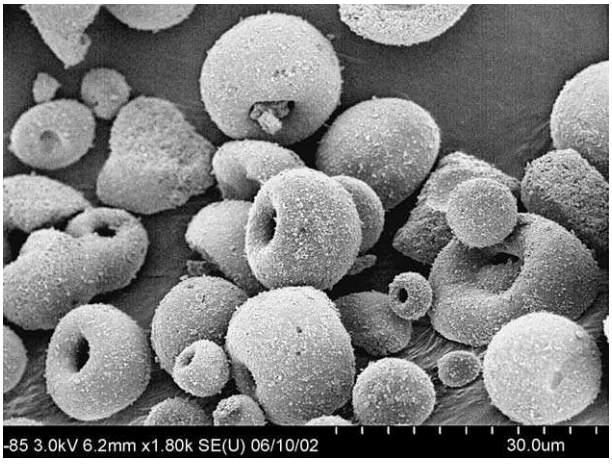

Fig. 1. Microscopic titania feedstock particles formed by the agglomeration of nanostructured particles of titania.

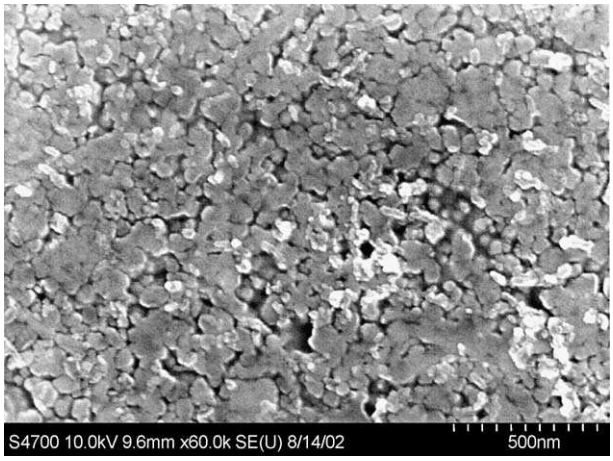

Fig. 2. Cross-section of a microscopic particle formed by the agglomeration of individual nanosized titania particles.

sprayed nanostructured and conventional feedstocks exhibited an overlapping of particle temperature and velocity distributions. The average particle temperature and velocity for the nanostructured particles were 1816±156 °C and 643±101 m/s, whereas, for the conventional particles, they were 1811±177 °C and 751±117 m/s. This is an interesting result because it ensures that, concerning in-flight particle characteristics, the nanostructured and conventional particles HVOF-sprayed arrived at the substrate with similar distributions of temperature and velocity; however, the overall average particle velocity for the conventional material is 17% higher.

Concerning the air plasma-sprayed particles, the results were as expected; that is, the average particle temperature was higher (2718±170 °C) than that of the HVOF-sprayed particles, and the particle velocity was lower (302±66 m/s). Consequently, the microstructural characteristics and mechanical properties of the air plasma-sprayed titania coating are expected to be significantly different from those of the HVOF-sprayed coatings.

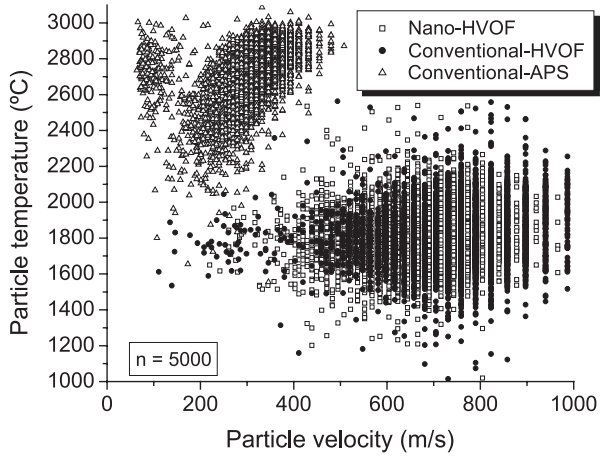

Fig. 3. Particle temperature versus particle velocity for the nanostructured and conventional titania feedstock particles HVOF-sprayed and for the conventional titania particles air plasma sprayed.

Table 2
Relative comparison of coating residual stress (coating thickness 530–580 μm)

Coating	Deflection (μm)	Residual stress
Nanostructured HVOF	−145	Compressive
Conventional HVOF	−406	Highly compressive
Conventional APS	−25	Slightly compressive

3.3. Residual stress

The results of residual stress can be found in Table 2. The three coatings (typical thickness (~550 μm) exhibited different levels of compressive residual stress. It is interesting to compare the two HVOF-sprayed coatings. They exhibited similar temperature distributions (Fig. 3), similar maximum coating temperature (~270 °C), similar deposition rate (~8 μm/pass) and similar thicknesses (~550 μm). However, the HVOF-sprayed coating made from the conventional feedstock exhibited a deflection 2.8 times higher than that of the HVOF-sprayed coating made from the nanostructured feedstock. Although the speed of the conventional particles was 17% higher than that of the nanostructured ones, it is not thought that this played a major role because the main source for residual stress levels in ceramic coatings is the mismatch of thermal expansion coefficient between the coating and the substrate [18].

3.4. Phase characterization

Figs. 4–6 show the XRD patterns of the three titania coatings. The patterns of the two HVOF-sprayed coatings are similar (Figs. 4, 5), with the same diffraction peaks for both patterns; rutile is the main phase, and anatase is the secondary one. However, the HVOF-sprayed coating made from the conventional feedstock exhibited some amorphous phase characterized by two humps at 2θ 25–30° and 53–57°.

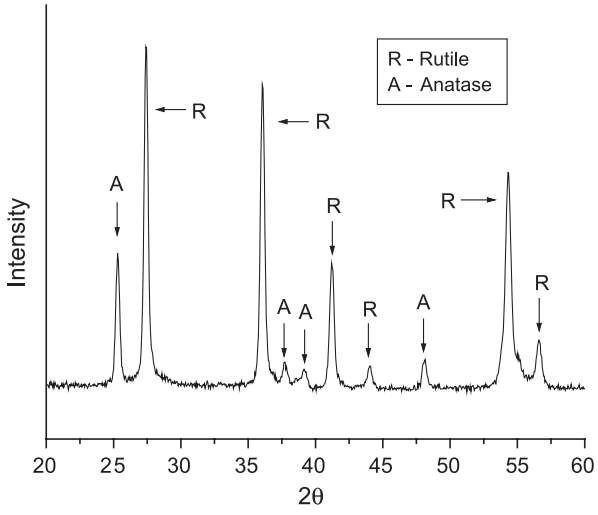

Fig. 4. XRD pattern of the HVOF-sprayed coating made from the nanostructured feedstock VHP-DCS (5–20 μm).

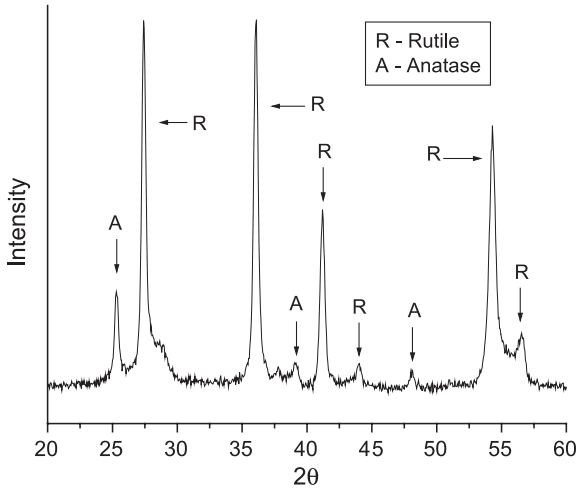

Fig. 5. XRD pattern of the HVOF-sprayed coating made from the conventional Flomaster feedstock.

The air plasma-sprayed coating made from the conventional feedstock exhibited rutile as the main phase (Fig. 6); however, it also exhibited amorphous humps, anatase/brookite and Magneli phases. When titania is heated in a reducing atmosphere (like the atmosphere of a plasma spray jet), it is easily reduced to lower valence oxides, such as the Magneli phases Ti_nO_{2n-1} (n=4 to 10) [3]. Therefore, the Magneli phase was observed in the air plasma-sprayed coating due to the high temperatures and reducing atmosphere of the plasma jet. The Magneli phases are probably not found in the HVOF-sprayed coatings due to the oxidizing effect of the HVOF flame, which impedes the loss of oxygen.

3.5. Abrasion resistance

Fig. 7 shows the volume loss for the coatings made from nanostructured and conventional titania feedstocks sprayed via HVOF and APS. Concerning the results for the HVOF-sprayed coatings, this work observed the same characteristics as those observed by Liu et al. [12]; that is, when spraying ceramics via HVOF, the abrasion resistance of the coatings exhibits a considerable improvement when compared to those of the air plasma-sprayed ceramic coatings. This behavior is probably associated with the high microstructural homogeneity of the HVOF-sprayed ceramic coatings [4,5].

Other characteristics also contribute to the superior abrasion resistance of the HVOF-sprayed ceramics. The porosity of the air plasma-sprayed coating was found to be 2.5±0.4%, whereas the porosity of the two HVOF-sprayed coatings was less than 1%. Porosity reduces the mechanical strength (or modulus of rupture) in ceramic materials for two reasons: pores (i) reduce the cross-sectional area across which the load is applied and (ii) act as stress concentrators. Porosity decreases the values of the mechanical strength of ceramic materials. It has been shown that the mechanical strength of some ceramic materials decreases exponentially with volume fraction of porosity [19]. Ceramic thermal spray coatings exhibit a bimodal distribution of porosity, with coarse pores (3–10 μm) and fine interlamellar pores (0.1 μm) [20]. It is thought that the high velocities attained by HVOF-sprayed particles tend to decrease the amount of coarse and interlamellar pores in the coating structure, therefore increasing its mechanical strength, which is paramount for producing abrasion resistant ceramic coatings.

From the results of Fig. 7, it is important to point out that, from a traditional air plasma-sprayed conventional titania coating to the HVOF-sprayed titania coating made from the nanostructured feedstock, there is a reduction in volume loss of 60% in the abrasion test, which is a considerable improvement.

Furthermore, when comparing the volume loss of the two HVOF-sprayed coatings, there is a reduction of volume loss

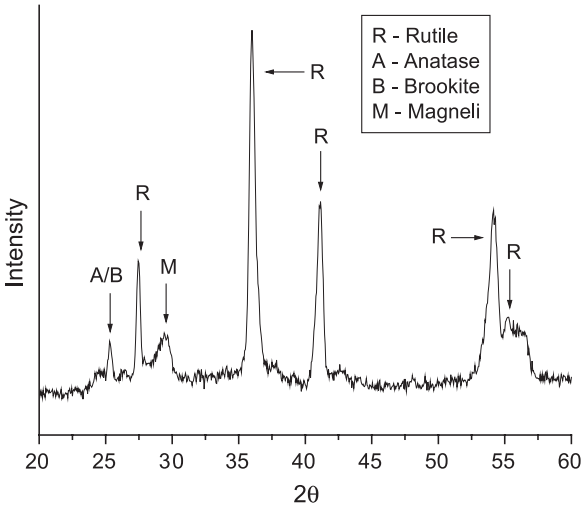

Fig. 6. XRD pattern of the air plasma-sprayed coating made from the conventional Metco 102 feedstock.

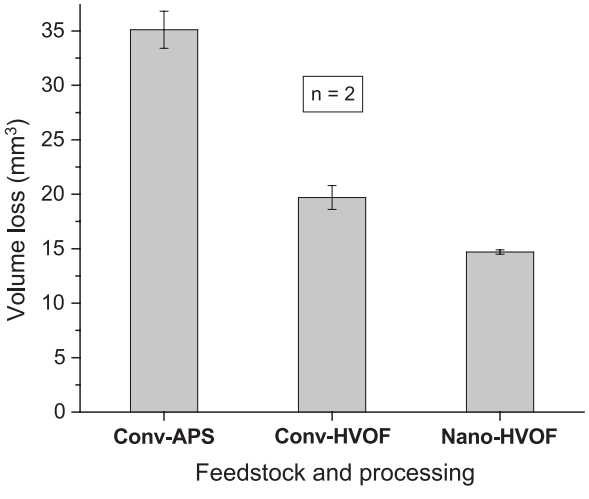

Fig. 7. Abrasion test result showing the volume loss for the coatings made from nanostructured and conventional titania feedstock powders sprayed via HVOF and APS.

of 25% in the abrasion test from the conventional to the nanobased coating, which is also an appreciable reduction. And it is thought that this volume loss reduction of 25% is closely associated with some "nanocharacteristics" of the coating because, as mentioned in the previous sections of this paper, the porosity, phase content and spraying/deposition characteristics of both HVOF-sprayed coatings were similar. Therefore, it is claimed that this difference or reduction of 60% in volume loss from the air plasma-sprayed conventional TiO_2 to the HVOF-sprayed nanostructured TiO_2 is mainly related to the HVOF processing (by reducing porosity) and to the nanocharacter of the coating.

It is important to point out that, when comparing the results of volume losses of Fig. 7 with the results of residual stress (Table 2), no significant relation is found between these properties. Higher or lower compressive residual stress levels did not translate into higher or lower abrasion resistance.

3.6. Nanostructure and microstructure

Figs. 8–10 show the microstructural features of the coatings made from the nanostructured and conventional titania feedstocks via APS and HVOF. All microstructures are uniform, mainly that of the HVOF-sprayed coating made from the nanostructured titania feedstock, which looks like a "bulk" microstructure not exhibiting any visible characteristics of the typical lamellar structure of thermal spray coatings. Another characteristic is observed for this coating, it is not possible to distinguish any nonmolten or semi-molten agglomerated nanostructured particles in the coating microstructure (Fig. 10).

It was mentioned in Section 3.1 that, in thermal spray coatings made from nanostructured feedstocks, nonmolten feedstock particles are surrounded by the particles that were melted during the spraying process, providing coating integrity [17]. However, when looking at the microstructure

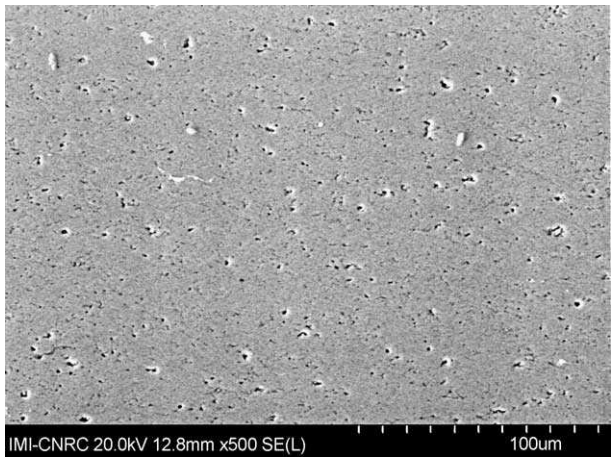

Fig. 9. Microstructure of the titania coating made from the conventional Flomaster feedstock by HVOF spraying.

of Fig. 10 taken at a low magnification (e.g., 500×), only particles that were fully melted during spraying are observed.

Fig. 11 shows a SEM picture (taken at 100,000×) of the HVOF-sprayed titania coating made from the nanostructured feedstock. It is possible to observe a nonmolten or partially molten particle (nanozone) with a diameter between 0.5 and 1 μm containing agglomerated nanostructured particles of titania with individual sizes less than 150 nm. This nonmolten zone (Fig. 11) resembles very well the morphology of the nanostructured feedstock particle (Fig. 2); therefore, Fig. 11 really represents a nonmolten or partially molten nanostructured feedstock particle embedded in the coating microstructure. It is important to notice that the nonmolten particle is very well embedded in the coating microstructure; that is, there are no filling defects or gaps between the molten and nonmolten zones of the coating as is normally observed in ceramic thermal spray coatings.

The zones containing agglomerated nanostructured particles, like the one shown in Fig. 11, were observed

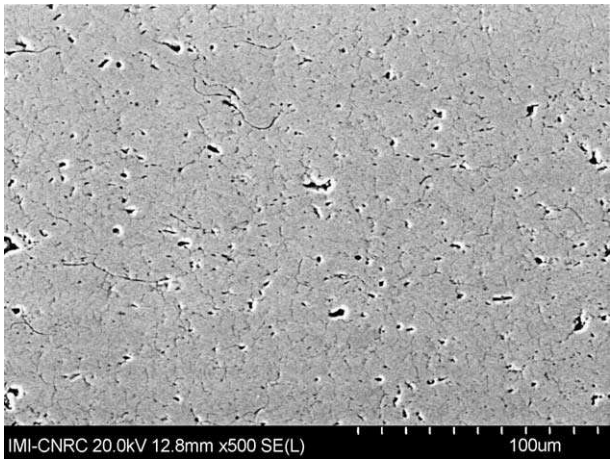

Fig. 8. Microstructure of the titania coating made from the conventional Metco 102 feedstock by air plasma spraying.

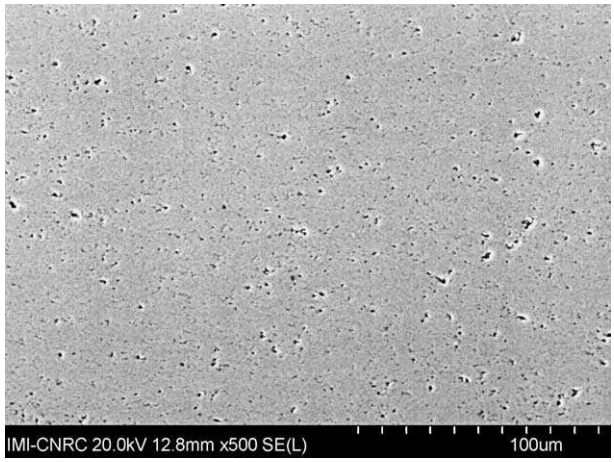

Fig. 10. Microstructure of the titania coating made from the nanostructured VHP-DCS (5–20 μm) feedstock by HVOF spraying.

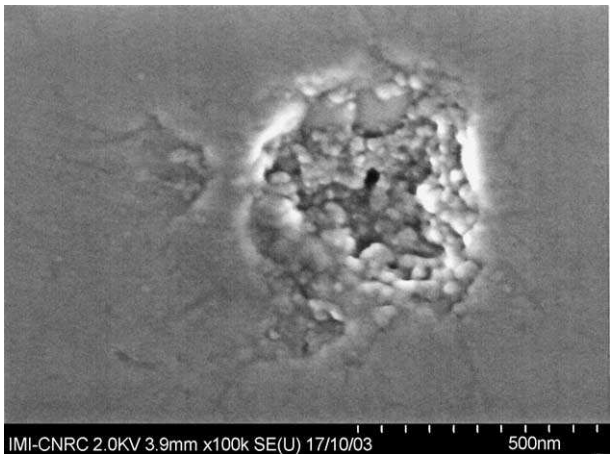

Fig. 11. A zone of agglomerated nanostructured titania particles in the HVOF-sprayed titania coating made of the nanostructured VHP-DCS (5–20 μm) feedstock.

randomly spread throughout the coating. These uniformly dispersed nanozones may be contributing to the significant gain in abrasion resistance observed in the coatings sprayed via HVOF using the nanostructured titania feedstock (Fig. 7). Consequently, the challenge now is to explain why and how these nanostructured particles are increasing the abrasion resistance of the HVOF-sprayed coating. This will be done in the next sections.

3.7. Hardness, crack propagation resistance and coating isotropy

Fig. 12 shows the hardness and crack propagation resistance for the titania coatings produced in this study. It is interesting to observe that all three titania coatings have similar values of Vickers hardness number (~850). Therefore, the superior wear behavior of the coating made from the nanostructured feedstock cannot be explained in terms of hardness. Based on the fact that the majority of the nanostructured and conventional particles embedded in the coating microstructure were fully molten during spraying, the hardness values of the three coatings are expected to be similar.

The results for the crack propagation resistance shown in Fig. 12 indicate that these coatings have very different behaviors. There is an increase of 13% in crack propagation resistance from the air plasma-sprayed to the HVOF-sprayed coatings made from conventional feedstocks. When comparing the HVOF-sprayed coating made from the nanostructured feedstock to the air plasma-sprayed coating made from the conventional feedstock, the value of crack propagation resistance almost doubles. Figs. 13–15 show the typical crack propagation behavior for the coatings produced in this study. It is possible to observe the significantly different crack propagation behavior of the HVOF-sprayed coating made from the nanostructured feedstock (Fig. 15). The cracks are shorter, and their propagation is more isotropic; that is, there are four cracks of approximately the same length emanating from the four corners of the Vickers indentation impression, which is a typical characteristic regularly observed for indentation toughness tests on isotropic ceramic and cermet bulk materials [13]. This crack pattern arises due to the isotropic microstructural nature that regular bulk materials exhibit.

On the other hand, the indentation cracks produced on the cross-section of regular ceramic and cermet thermal spray coatings normally exhibit a somewhat different pattern, which is associated with the anisotropic microstructure [20] of these coatings. In these materials, the following crack pattern is generally produced: two dominant cracks parallel to the substrate surface emanate from (or near) the corners of the Vickers indentation impression [21–23], like the ones observed in Figs. 13 and 14.

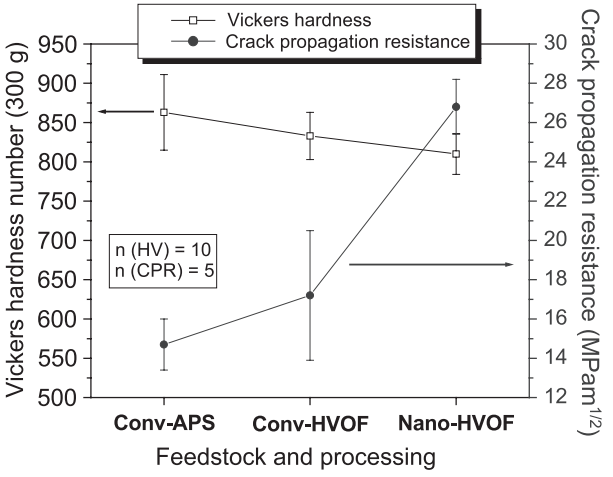

Fig. 12. Vickers hardness and crack propagation resistance for the coatings made from nanostructured and conventional titania feedstocks sprayed via HVOF and APS.

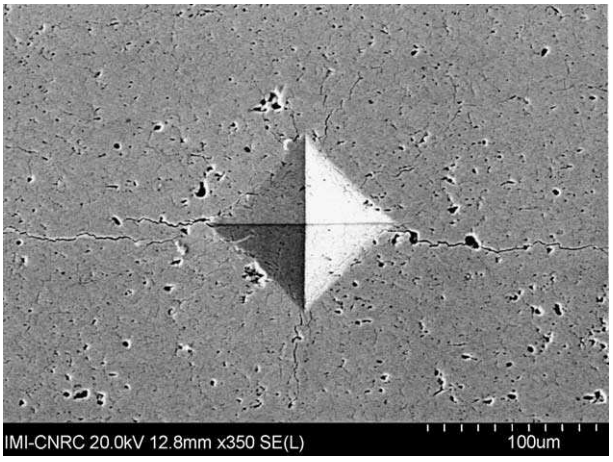

Fig. 13. Crack propagation via Vickers indentation (5 kgf) on the cross-section of the air plasma-sprayed coating made from the conventional Metco 102 feedstock.

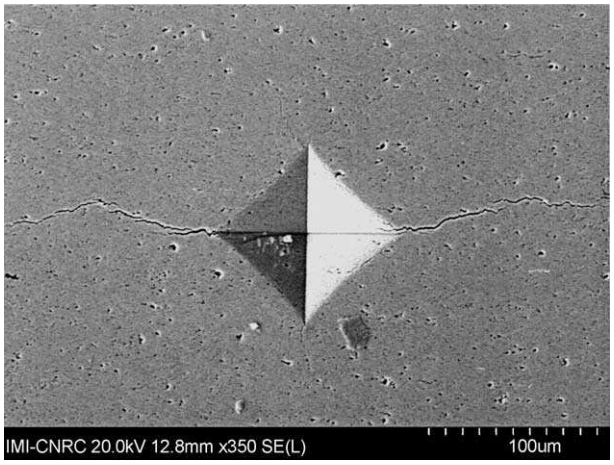

Fig. 14. Crack propagation via Vickers indentation (5 kgf) on the cross-section of the HVOF-sprayed coating made from the conventional Flomaster feedstock.

It has been suggested in earlier work [4,5] that ceramic thermal spray coatings may exhibit isotropic characteristics of microstructure and mechanical properties when their microstructures are very dense and uniform, as that shown in Fig. 10. A key factor in producing such structures is ensuring that the sprayed particles have a narrow particle size distribution and fine cut (e.g., 5–20 μm), which results in a more uniform particle heating during spraying.

It is important to point out that the crack propagation resistance is an indirect measurement of toughness. Therefore, toughness is the agent responsible for the higher abrasion resistance (and mechanical strength) of the HVOF-sprayed coatings, mainly, for the HVOF-sprayed coating made from the nanostructured feedstock. As previously discussed, there are nanozones uniformly dispersed throughout the coating microstructure. The question that has to be answered is if these nanostructured zones are really causing this increase in crack propagation resistance.

Fig. 16a shows a Vickers indentation impression (1 kgf) in the cross-section of an HVOF-sprayed nanostructured titania coating. It is possible to observe cracks coming out from the corners of the indentation impression. Fig. 16b shows the tip of the right crack of the indentation impression. It shows how the nanostructure zones are interacting with a crack. When the indentation crack tips in the HVOF-sprayed coating made from the nanostructured titania feedstock are analyzed at high magnification, it is observed that the cracks are often arrested by the nanostructured zones (Fig. 16b). It is important to point out that the nonmolten or partially molten particle of Fig. 16b, as that of Fig. 11, are very well embedded in the coating microstructure; that is, they do not exhibit filling defects or gaps between the molten and nonmolten zones of the coating. Therefore, when a propagating crack reaches the nonmolten particle, it does not skirt the nonmolten particle along the gap, which would be the less resistant path. For conventional materials, the cracks propagate through the splat boundaries and do not have nanozones to impede their

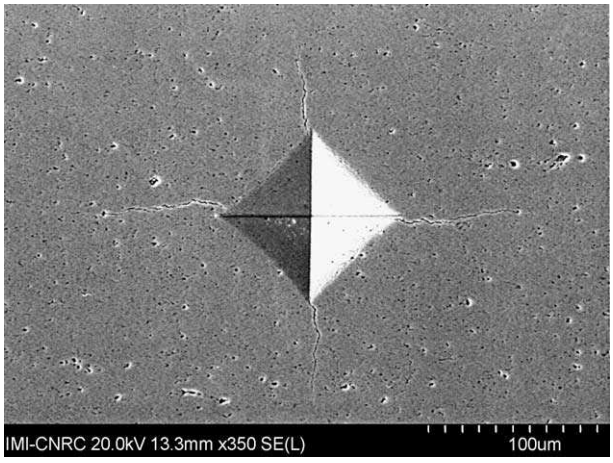

Fig. 15. Crack propagation via Vickers indentation (5 kgf) on the cross-section of the HVOF-sprayed coating made from the nanostructured VHP-DCS (5–20 μm) feedstock.

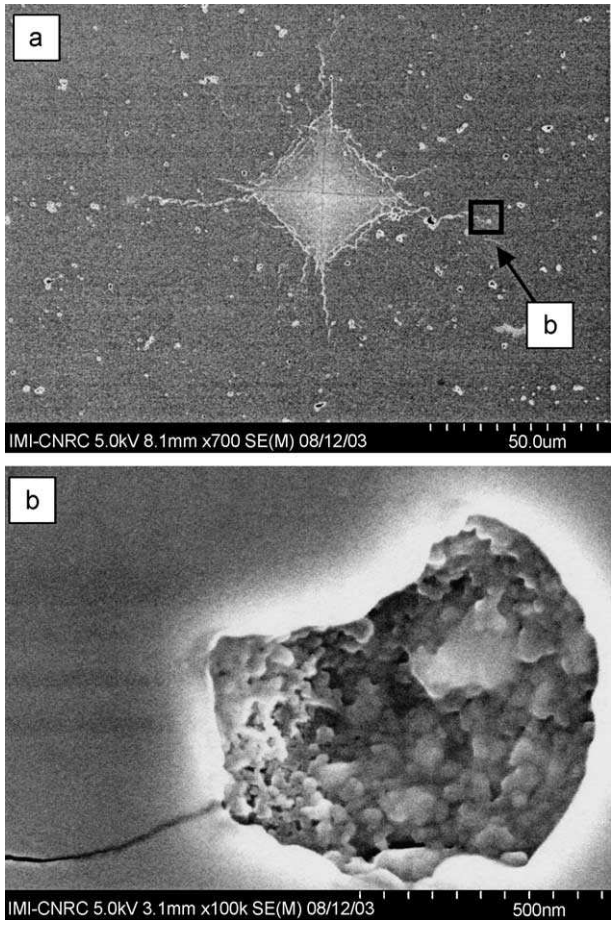

Fig. 16. Vickers indentation impression (1 kgf) in the cross-section of the HVOF-sprayed nanostructured titania coating (a) and the indentation crack tip being arrested by a zone of nanostructured particles (b).

path; therefore, a crack propagates until its energy is not enough to break the weak splat boundaries.

Based on the experimental observations of (Figs. 10, 11, 15 and 16), it is suggested that the HVOF-sprayed titania coating made from the nanostructured feedstock is exhibiting isotropic characteristics of microstructure and mechanical properties; that is, the coating is behaving as a bulk material. Nanostructured zones (Figs. 11 and 16) are uniformly spread throughout the coating microstructure, acting as crack arresters, toughening the coating. Such a toughening mechanism was suggested by references [9,10,24,25] in a study of mechanical properties of nanostructured related ceramic thermal spray coatings.

Some of the characteristics of the toughening mechanism caused by the presence of these nanostructured zones are thought to be similar to those found in toughened bulk ceramics, where fine particles (submicron to a few microns in size) are uniformly dispersed in the ceramic matrix structure [26].

3.8. Bond strength

The bond strength results for the three titania coatings produced in this study can be found in Fig. 17. The HVOF-sprayed titania coatings made from the nanostructured feedstock exhibited a bond strength 65% higher than the bond strength of the air plasma-sprayed conventional feedstock coating. It has been reported in the literature that HVOF-sprayed coatings tend to exhibit higher bond strength levels than those of air plasma-sprayed coatings [18]. These higher values of bond strength are probably associated with the higher particle velocities attained by the HVOF-sprayed particles when compared to those of air plasma-sprayed particles (Fig. 3). However, the HVOF-sprayed coating made from the conventional feedstock exhibited the lowest bond strength of all three coatings.

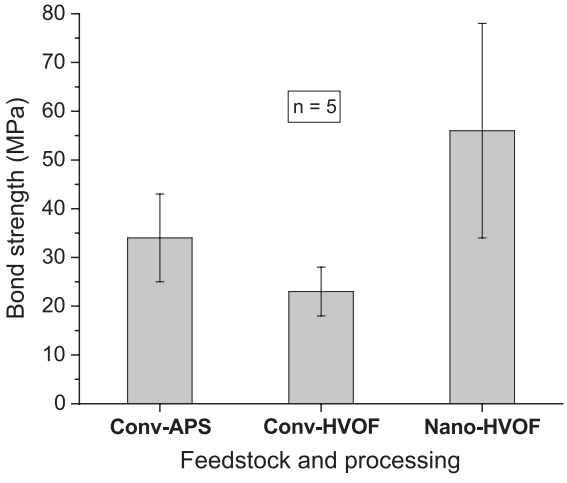

Fig. 17. Bond strength for the coatings made from nanostructured and conventional titania feedstock powders sprayed via HVOF and APS.

4. Conclusions

- In this work on nanostructured and conventional titania feedstocks sprayed by HVOF and APS, it was found that there is a decrease in volume loss of 60% in the abrasion test and an increase in bond strength of 65% from the traditional air plasma-sprayed coating made from a conventional feedstock to an HVOF-sprayed coating made from a nanostructured feedstock.
- The two HVOF-sprayed coatings (from a nanostructured and conventional feedstock) exhibited similar distributions of particle temperature and velocity, porosity, hardness, phase content, maximum coating temperature and deposition rate. Therefore, for the two HVOF-sprayed coatings, the superior abrasion resistance of the coating made from the nanostructured feedstock is considered related to the nanocharacter of the feedstock.
- The overall reduction of volume loss of 60% in the abrasion test from the air plasma-sprayed coating made from the conventional feedstock to the HVOF-sprayed coating made from the nanostructured feedstock is related to two main factors: (i) the lowering of coating porosity (via HVOF processing), which increases the mechanical strength of the ceramic coating, and (ii) the agglomerated nanoparticles distributed within the coating.
- Hardness properties alone cannot be used for explaining the higher abrasion resistance of the HVOF-sprayed coating made from the nanostructured feedstock. The three coatings studied in this work exhibited similar hardness values; however, the HVOF-sprayed coating made from the nanostructured feedstock exhibited the highest crack propagation resistance.
- The HVOF-sprayed nanostructured coatings made from the nanostructured feedstock exhibited very dense and uniform microstructural characteristics. A lamellar structure is not evident. This coating also exhibited isotropic characteristics of crack propagation under Vickers indentation. Therefore, this coating exhibits characteristics of bulk isotropic materials.
- The zones of agglomerated nanostructured titania particles (nonmolten particles) are randomly dispersed and very well embedded within the coating microstructure.
- It is thought that the enhanced crack propagation resistance of the HVOF-sprayed titania coating made from the nanostructured feedstock originates from the randomly dispersed nanostructured zones in the dense isotropic-like structure. The nanostructured zones act as crack arresters by blunting or branching crack tips.

Acknowledgements

This research was based in part on a project funded by Altair Nanomaterials (Reno, NV, USA). The authors want to thank Altair Nanomaterials for encouraging the publication

of these results. The authors also want to thank S. Belanger and F. Belval for APS and HVOF spraying, M. Lamontagne for the DPV2000 measurements, E. Poirier for metallography/bond strength tests and M. Thibodeau for XRD spectra and SEM pictures.

References

[1] Metco 102 Titanium Dioxide Powder—Technical Bulletin #10-092, Sulzer-Metco, Westbury, NY, USA.
[2] P. Fauchais, in: S.J. Schneider Jr. (Ed.), Engineering Properties of Single Oxides, Engineered Materials Handbook, Ceramic and Glasses, vol. 4, ASM International, Materials Park, OH, USA, 1991, p. 202.
[3] M. Miyayama, K. Koumoto, H. Yanagida, in: S.J. Schneider Jr. (Ed.), Engineered Materials Handbook, Ceramic and Glasses, vol. 4, ASM International, Materials Park, OH, USA, 1991, p. 748.
[4] R.S. Lima, B.R. Marple, J. Therm. Spray Technol. 12 (2) (2003) 240.
[5] R.S. Lima, B.R. Marple, J. Therm. Spray Technol. 12 (3) (2003) 360.
[6] C.C. Koch, D.G. Morris, K. Lu, A. Inoue, MRS Bull. (1999 February) 54.
[7] R. Vaßen, D. Stover, J. Mater. Process. Technol. 92–93 (1999) 77.
[8] Y. Lu, P.K. Liaw, J. Met. (2001 March) 31.
[9] M. Gell, E.H. Jordan, Y.H. Sohn, D. Goberman, L. Shaw, T.D. Xiao, Surf. Coat. Technol. 146–147 (2001) 48.
[10] E.H. Jordan, M. Gell, Y.H. Sohn, D. Goberman, L. Shaw, S. Jiang, M. Wang, T.D. Xiao, Y. Wang, P. Strutt, Mater. Sci. Eng., A 301 (2001) 80.
[11] G.E. Kim, J. Walker Jr., J.B. Williams Jr., U.S. Patent No. 2003/0049449 A1, 13 March, 2003.
[12] Y. Liu, T.E. Fischer, A. Dent, Surf. Coat. Technol. 167 (2003) 68.
[13] G.R. Anstis, P. Chantikul, B.R. Lawn, D.B. Marshall, J. Am. Ceram. Soc. 64 (9) (1981) 533.
[14] Standard Test Method for Measuring Abrasion using the Dry Sand/Rubber Wheel Apparatus, ASTM Standard G65-00. ASTM, West Conshohocken, PA, USA.
[15] Standard Test Method for Adhesion or Cohesion Strength of Thermal Spray Coatings, ASTM Standard C 633-01. ASTM, West Conshohocken, PA, USA.
[16] J.P. Sauer, P. Sahoo, in: C.C. Berndt, K.A. Khor, E.F. Lugscheider (Eds.), Thermal Spray 2001: New Surfaces for a New Millenium, ASM International, Materials Park, OH, USA, 2001, p. 791.
[17] R.S. Lima, A. Kucuk, C.C. Berndt, Mater. Sci. Eng., A 313 (2001) 75.
[18] L. Pawlowski, The Science and Engineering of Thermal Spray Coatings, John Wiley & Sons, Chichester, West Sussex, England, 1995.
[19] W.D. Kingery, H.K. Bowen, D.R. Uhlmann, Introduction to Ceramics, 2nd edition, John Wiley & Sons, New York, NY, USA, 1976, p. 809.
[20] R. McPherson, Surf. Coat. Technol. 39/40 (1989) 173.
[21] P. Ostojic, R. McPherson, Mater. Forum 10 (4) (1987) 247.
[22] E. Lopez Cantera, B.G. Mellor, Mater. Lett. 37 (1998) 201.
[23] S. DePalo, M. Mohanty, H. Marc-Charles, M. Dorfman, in: C.C. Berndt (Ed.), Thermal Spray-Surface Engineering via Applied Research, ASM International, Materials Park, OH, USA, 2000, p. 245.
[24] H. Luo, D. Goberman, L. Shaw, M. Gell, Mater. Sci. Eng., A 346 (2003) 237.
[25] G.E. Kim, J. Williams Jr, J. Walker Jr., PDF file in Proceedings of the 6th International Conference on Nanostructured Materials (Nano 2002), June 16–21, 2002, Orlando, FL, USA, 2002, 6 pp.
[26] H. Zhang, D. Wang, S. Chen, X. Liu, Mater. Sci. Eng., A 345 (2003) 118.